

Structural and functional characterization of protein isolate from *Lepidium sativum* with antioxidant and antidiabetic activities

Deepak Kadam (✉ deepakskadam90@gmail.com)

Institute of Chemical Technology

Aayushi Kadam

Anatek Services PVT LTD

Kanchanlata Tungare

D. Y. Patil Deemed to be University, CBD-Belapur

Priyamvada Arte

D. Y. Patil Deemed to be University, CBD-Belapur

S. S. Lele

Institute of Chemical Technology

Research Article

Keywords: *Lepidium sativum* protein isolate (LSPI), Structural characterization, Functional properties, therapeutic herb, antioxidant

Posted Date: September 14th, 2022

DOI: <https://doi.org/10.21203/rs.3.rs-2053419/v1>

License:   This work is licensed under a Creative Commons Attribution 4.0 International License.

[Read Full License](#)

Abstract

The extraction of protein from *Lepidium sativum* (LS) seed cake was optimized to obtain a yield of 18.32% at an alkali concentration of 0.16 M, buffer to sample ratio of 1/25 (w/v), a period of extraction of 15 min at 25°C. The physicochemical attributes, amino acid composition as well as functional properties of *Lepidium sativum* protein isolate (LSPI) were evaluated. Determining amino acid composition indicated that the isolated protein is a decent source of dietary essential amino acids with 41.36% being essential amino acids. The secondary structure of LSPI was mainly constituted by β -structures. Further, the protein isolate exhibited an excellent solubility profile at basic pH. Experimental data obtained from physicochemical analysis implies that the LSPI had excellent water holding and oil absorption capacity, emulsification property, foaming capacity and stability. LSPI exhibited significant antioxidant, anti-diabetic and protein digestibility activities making them an excellent candidate for nutritional food development.

1. Introduction

The demand for plant-based proteins has surged in recent years owing to their association with multiple health benefits and nutritional advantages [1]. It serves as an effective substitute to high quality animal proteins that presents environmental sustainability challenges. Production of 1 kg high quality animal protein entails consumption of 6kg plant protein to livestock which further leads to depletion of land and water resources along with emission of greenhouse gases through livestock agriculture [2]. An extensive application of plant derived protein can effectively minimise the detrimental environmental issues and at the same time can extend an adequate amount of protein to the population. Compared to the animal-derived protein, plant-based protein is contemplated as a safe, economical and environmentally sustainable dietary source of proteins [3]. These proteins have immense potential to serve as nutritional and functional food ingredients and thus become a trending area of research. Also, the market value of protein ingredient that was estimated to be 38 billion USD in 2019, is expected to soar by 9.1% in coming years thereby unfolding the need of exploring additional plant protein sources and better extraction procedures [1].

Amongst the various vegetable sources studied for isolating proteins, plant seed waste has gained lot of attention as it serves as an effective alternative and supports waste utilisation [4]. Plant seeds, especially the oilseeds are extracted only for the fat content and the rest is regarded as waste. These seed cakes are rich in proteins, carbohydrates, and fibres. Extraction of protein from these seed cake can be of additional value and make the process economically viable [5].

Garden cress (*Lepidium sativum*) is a fast growing, annual, edible herb that belongs to the *Brassicaceae* family and is found in the temperate region of the world [6]. It is considered to be among the chief therapeutic herbs that are traditionally used by rural and tribal people. The seeds are bitter, aphrodisiac, depurative, diuretic, tonic, aphrodisiac, thermogenic antiscorbutic, antihistaminic and ophthalmic [7]. They are used in the curing wild range of disorder such as skin disease, asthma, leprosy, hepatopathy,

scurvy and seminal weakness (Kadam et al., 2018). The seeds are brown in colour and contain the maximum amount of mucilage. It harbours 43.5% of carbohydrate, 23.4% of fats, and 22.75% of protein (w/w) indicating it to be a rich source of nutrients [7, 9]. However, studies that are reported on *Lepidium sativum* seed are mainly focused on its oil and mucilage content, with little or no information on protein content. Further, as compared to carbohydrates and fats, seed dietary proteins exhibit its specific nutritious property with significant medicinal value and contain a substantial amount of essential amino acids [10]. All these findings indicate that *Lepidium sativum* seed has a potential to meet the demand for the plant-based protein with specific functionality in the food industry. To the best of our knowledge, no significant studies have been conducted concerning the isolation and characterization of Cress seed protein.

Therefore, the objective of this work was to optimize the extraction procedure of Cress seed protein isolate by means of Response Surface Methodology (RSM). The physicochemical characteristics and functional properties of the *Lepidium sativum* seed protein isolate (LSPI) were also investigated.

2. Material And Method

2.1. Material

Garden cress (*Lepidium Sativum*) seed was obtained from the local market, Mumbai, India. The cleaned seeds were rendered free of dust, stone, and were broken manually. The cleaned seeds were then packed in a polyethylene bag and refrigerated until further use.

2.2. Sample Preparation

The garden cress seeds were grounded and extracted for oil in a Soxhlet apparatus with solvent n-hexane for 5 h. Followed by drying of the defatted seed flour at room temperature at (~ 27°C). Defatted seed flour was then grounded again and passed through a 60-mesh sieve.

2.3. Protein Extraction from black cumin seed

The cress seed protein extraction was carried out as reported by Siow & Gan, 2014 with minor modifications. Briefly, defatted seeds meal was extracted in water with a seed to a solvent ratio of 1:20 – 1:50 at alkali concentration of 0.1-0.3M. The buffer was preheated to a proposed temperature (20–50°C) prior to the seed meal addition. The seed-water slurry was mixed throughout the extraction period (15-75min) with constant agitation at 500rpm. Subsequently, the mixture was centrifuged at 8000 × g at 4°C for 20 min, followed by pH adjustment of the supernatant collected to the isoelectric point of the protein. The resulting slurry was centrifuged again and the sediment so obtained was vacuum dried and stored in a refrigerator until further use. Soluble protein content was estimated using Bradford assay.

2.4. Proximate analysis

The moisture, ash value, crude protein (N 6.25) and the fat content of the seed was determined according to the Association of Official Analytical Chemists (AOAC, 2005) method. Carbohydrate content was

obtained by the difference of the other components (AOAC, 2005).

2.5. Experimental design

Initially, the primary range of extraction variables was determined by the method of a single factor at a time. Further, the extraction parameters were optimized via response surface methodology (RSM) using central composite design (CCD) of four independent variables; alkali concentration (x_1), the sample to buffer ratio (x_2), time (x_3) and temperature (x_4) of extraction. The range of independent variables with the levels examined in this work are given in Table 1 and their coded levels: -2, -1, 0, 1, 2 in Table 2.

$$x = \frac{(X_i - X_0)}{\Delta X}$$

1

As given in Table 2, the experimental design consisted of 30 random combination points, 16 are the factorial points, 8-star points, and 6 central points. Star points were provided to estimate the pure quadratic effect in the model. The response function (Y) was protein content, tannin content, total phenol content.

The second-order polynomial model below, explains the relationship between independent and response variables.

$$Y = \beta_0 + \sum_{i=1}^3 \beta_i X_i + \sum_{i=1}^3 \beta_{ii} X_i^2 + \sum_{i=1}^2 \sum_{j=i+1}^3 \beta_{ij} X_i X_j$$

2

Where, Y represents the response variable; β_0 is a central point (constant), β_i , β_{ii} , β_j are the linear, quadratic and interaction term regression coefficients. X_i and X_j represent independent variables. The fitted experimental data in the polynomial model generated 3-D response surface and contour plots that visualize the interaction among experimental levels of every factor and response [12].

2.6. Characterization of protein isolate

2.6.1. Sodium dodecyl sulfate-polyacrylamide gel electrophoresis (SDS-PAGE)

SDS-PAGE of the LSPI was carried out by the method of Vishwasrao et al., 2017 with some modification. The analysis was carried out employing 12% resolving and 4% stacking polyacrylamide gel (29:1, acrylamide: bisacrylamide) and β -mercaptoethanol as reducing agent using Mini-Protean III Cell (Bio-Rad, USA) apparatus at a voltage of 100V at 24°C for 4 h. A mixture of the mid-range marker proteins (20–300 kDa) was used as a standard. Silver nitrate staining of the gel followed by imaging was done for detection (Imager ChemiDoc™ XRS+).

2.6.2. Amino acid Composition

Determination of the amino acid composition of the isolated protein was done according to the method of Gratzfeld-Huesgen, 1999 with some modifications. Hydrolysis of the defatted sample (100 mg) was done by dissolving in 5 mL of 6N HCl and exposing it to 110°C for 24 hr with intermittent shaking for every 1 hr. The hydrolyzed sample was centrifuged at 1372 g for 15 min, followed by neutralization of the supernatant with 1N NaOH and dilution in the ratio of 1:100 of volume with milli-Q water. The amino acids sample was then analyzed by RP-HPLC analysis (Agilent 1100, Agilent Technologies Co. Ltd., Palo Alto, CA, USA). The column used was Agilent (Zorbax) 300SB-C18 (4.6 x 250mm).

2.6.3. Fourier transform infrared spectroscopy (FTIR)

Detection of preliminary structures of LSPI was carried out using FTIR spectrometry (EQUINX55, Bruker, Germany) with 4 cm⁻¹ resolutions in the range of 4000–500 cm⁻¹.

2.6.4. Scanning Electron Microscopy (SEM)

Morphological features of the lyophilized LSPI were analyzed using SEM (JSM- 7600F, Jeol Ltd., Japan). Samples were fixed on copper stubs, covered with a platinum sputter and analyzed at 15 kV.

2.6.5. XRD analysis

The crystal structure of the LSPI was studied by the Rigaku® X-ray diffractometer (RINT2000, Tokyo, Japan) at a voltage of 40 kV and 30 mA. Detection of the scattered radiation was done in the angular range (2θ) of 5–80° with a scanning speed of 2° min⁻¹.

2.6.6. Thermal analysis

The DSC analysis of LSPI was carried out using the DSC-60 (Shimadzu Scientific Instruments, Kyoto, Japan) instrument equipped with a TA 60 WS detector and computer-aided data analysis. About 4 mg weighing sample was sealed hermetically in standard aluminum DSC pan and scanned between 35 and 200°C with 10°C /min heating rate.

2.6.7. Antioxidant property

Antioxidant activity of the LSPI was evaluated in terms of DPPH radical scavenging activity [15, 16], Ferric reducing antioxidant power (FRAP) and ABTS radical scavenging assay [16, 17].

2.6.8. *In vitro* protein digestibility and α-Amylase inhibition activity of LSPI

In-vitro digestibility of LSPI was determined according to the method of Phongthai et al., 2016. The α-amylase inhibition assay was performed according to the DNSA method described by Mehta et al., 2016. The reaction mixture consisted of 0.02M sodium phosphate buffer (pH 6.9) containing 6mM sodium chloride (500μL), 0.04 units of pancreatic α-amylase and the extract was pre-incubated at 37°C for 10 min. Followed by addition of 500μL of 1% (v/v) starch solution and was kept undisturbed for 15 min at

37°C. The subsequent reaction termination was performed by adding 1 mL of DNSA reagent and heating in a boiling water bath for 5 min. The contents were brought to room temperature and the absorbance was read at 540nm. The control tube demonstrating 100% enzyme activity did not contain the extract.

2.7. Functional properties

2.7.1. Solubility of Protein

The influence of ionic strength on the aqueous solubility of LSPI was assessed as a function of pH and NaCl concentration. Protein sample (100 mg) was combined with 10 mL of deionised water in a dilution of (0, 0.5, 1.0, 1.5 and 2.0 M) NaCl solutions adjusted to different pH levels (pH 2–11). The solutions were incubated for an hr at 20°C with continuous stirring and then centrifuged at 11,200 g for 15 min. Subsequently, filtration of the supernatant separated with a 0.22 µm syringe filter and the protein content estimation by Bradford method.

2.7.2. Determination of bulk density, water holding, and oil absorption capacity

The bulk density of LSPI was gauged by observing the volume of a known mass of the sample. A calibrated measuring cylinder was weighed (W_1) and filled with 10 mL of LSPI sample. The setup was placed without any disturbance and space between the particles were eliminated by gently tapping the cylinder. Then sample volume was taken and weighed as W_2 . By calculating the difference between W_1 and W_2 , the bulk density of LSPI was determined as g/mL [20].

The water holding capacity (WHC) of LSPI was evaluated using the method described by Timilsena et al., 2016. An aqueous solution of LSPI sample (1%) was stirred for 30 s and kept undisturbed for 30 min at 25°C. Successive centrifugation of the solution at 11,200 g for 15 min at 25°C was performed and the mass of the sediment obtained was noted. The WHC was calculated and expressed as mass (g) of water per unit of mass (g) of protein (LSPI)

Oil absorption capacity (OAC) of LSPI was evaluated similarly using sunflower oil and was expressed as mass (g) of trapped oil per unit mass (g) of LSPI.

2.7.3. Emulsifying activity index (EAI) and emulsion stability (ES)

EAI and ES index of LSPI was determined as a function of concentration and pH using the method as referred by Hou et al., 2017 with some adaptations. In this method, 10 mL sunflower oil whose pH was adjusted to specific values (3–11), was mixed with 50 mL of 0.1, 0.15 and 0.2% (w/v) of LSPI solution. The mixture was then homogenized at 4000 rpm for 3 min. Approximately 50 µl of emulsion aliquots were drawn out from the bottom of the beaker at 0 and 10 min of homogenization. Further 5 mL of 0.1% sodium dodecyl sulfate (SDS) solution was added to the aliquots and the absorbance was recorded at

500 nm using UV-Vis spectrophotometer (UV-1800 Shimadzu). With the absorbance measured at 0 min (A_0) and 10 min (A_{10}) after emulsion formation, EAI and ES were calculated as,

$$EAI(m^2/g) = \frac{(2 \times 2.303 \times A_0 \times N)}{(\rho \times \phi \times 10,000)}$$

3

$$ES (min) = \frac{A_0 \times 10}{A_0 - A_{10}}$$

4

Where N is the dilution factor, ϕ is the oil volumetric fraction (0.25) and ρ is protein concentration (g/mL).

2.7.4. Foaming capacity (FC) and Foaming stability (FS)

FC and FS were measured according to the protocol of Timilsena et al., 2016 with some minor modifications. To evaluate the FC, dispersion of the LSPI sample in 50 mL of Milli-Q water (0.03, 0.06 and 0.09%) was made and adjusted to specific pH levels (3–11). The foam was then formed by means of a mechanical homogenizer at 4000 rpm for 3 min at $25 \pm 2^\circ\text{C}$. Volume was logged pre and post whipping in a 100 mL graduated cylinder.

$$FC (\%) = \frac{(V_2 - V_1)}{V_1} \times 100$$

5

where V_1 and V_2 (mL) are the volumes of protein dispersion and dispersion plus the foam in mL respectively.

Stability of the foam (FS) was determined as a measure of the total volume after 10, 20 and 30 min of the foam formation as,

$$FS (\%) = \frac{(V_2 - V_3)}{(V_2 - V_1)} \times 100$$

6

where V_3 is the final volume (mL) after 10, 20 and 30 min of foam formation.

2.8. Statistical analysis

The experiment was performed in triplicate and expressed as a Mean \pm Standard deviation. The result was subjected to variance analysis using Tukey's test that was conducted using IBM® SPSS® version 18.0 at 95% significance level ($p < 0.05$).

3. Result And Discussion

Garden cress seeds possess several nutritious and medicinal properties like linolenic acid, amino acid and dietary fibers that are claimed to be used in many foods, nutraceutical, pharmaceutical, and cosmeceutical industries. Despite harbouring superior health-promoting constituents that can be extended to several application, their utilization is very limited and restricted to only extraction of fatty acid. Hence, the current study was focused on extraction, optimization, characterization and functional properties of protein content.

3.1. Proximate analysis of *Lepidium sativum* seed cake

Table 1 shows the proximate composition of *Lepidium sativum* seed cake. Protein content in the seed meal flour was found to be 28.25 g/ 100g which is considered to be adequate for protein recovery.

3.2. Extraction Optimization

The effect of four extraction parameters, alkali concentration (X_1), buffer to sample ratio (X_2), extraction temperature (X_3) and extraction time (X_4) on the yield of cress seed protein was analyzed using CCD design (Fig. 1). Protein yield (g/100g) was selected as a response function. In addition, shorter extraction time, a minimum buffer to sample ratio was used to optimize the protein yield. Also, from the industrial perspective, reduction in process waste and energy consumption would bring cost benefits while keeping the protein yield maximum. The experimental design had a total of 30 runs for protein yield optimization and associated experimental and predicted values are presented in Table 2. The result reveals that the experimental protein yield differed from the 14.65 to 21.11 g/100g under different experimental condition. The maximum protein yield (21.11 g/100g) was obtained under the tested condition of $X_1 = 0.2$, $X_2 = 43.47$, $X_3 = 30$, $X_4 = 60$.

3.3. Model fitting

Analysis of variance (ANOVA) of the independent variable was executed to assess the significance of model coefficients as given in Table 3. Statistical data reveals that the influence of the quadratic model was significant ($p < 0.0001$). The fitted response surface quadratic model for protein yield given in Eq. 7. Result reveals greater influence on the yield of protein was in linear term of alkali concentration (X_1), buffer to sample ratio (X_2), extraction temperature (X_3), extraction time (X_4) followed by quadratic term of alkali concentration (X_1^2), buffer to sample ratio (X_2^2), extraction temperature (X_3^2), extraction time (X_4^2) and interaction term of X_1X_4 . On the other hand, interaction terms of X_1X_2 , X_1X_3 , X_2X_3 , X_2X_4 , and X_3X_4 were not significant.

$$\begin{aligned} \text{Yield} = & 18.18 - 2.05 \times X_1 - 5.57X_2 - 1.17X_3 + 2.88X_4 - 6.96X_1^2 - 5.71X_2^2 - \\ & 2.46X_3^2 - 2.91X_4^2 - 0.57X_1X_2 + 0.44X_1X_3 + 2.6X_1X_4 - 0.15X_2X_3 - 0.64X_2X_4 + \\ & 0.059X_3X_4 \end{aligned}$$

As is shown in Table 3, the non-significant lack of fit further validated the model ($p > 0.05$) measuring the failure of the model at points which were not incorporated in regression [11]. Figure 2, depicted the linearity between the predicted and experimental value of protein yield. Values of the coefficient of determination ($R^2 = 0.933$), implied that the model reasonably fitted well and was adequate to represent the experimental data. Adjusted determination coefficient indicates an excellent correlation between experimental and predicted value ($R_{adj}^2 = 0.87$). The coefficient of variation (CV) of the model was estimated at 3.71% and it signifies the reproducibility of the model.

3.4. Interpretation of the 3D-surface response graph and contour plot

RSM was employed to visualize the main and interactive effect of independent variables on response through 3D response surface plots and contour plots (Fig. 2). It was observed that extraction temperature and buffer to meal ratio influenced the protein yield in a quadratic manner. Under extraction conditions, temperature of 30°C and alkali concentration of 0.18M gave maximum yield of protein with a constant buffer to meal ratio of 43.47/1(v/w) for 40 min. A protein yield was increased with an increase in alkali concentration but the increase in extraction temperature did not show any significant effect. The result so obtained corroborated with the study executed by Sonawane & Arya, 2017.

3.5. Verification of models

Verification of the model was performed for predicting the optimum response value which was validated by the recommended environment. According to energy conservation and attainability of the experiment, with a special recipe of extraction parameters, the protein yield was optimized. The predicted value of protein yield that is 19.09 g/100g corresponded to alkali concentration of 0.17 M, buffer to meal ratio of 45/1 (v/w), at 26°C for 42.86 min. The experimental value of 18.32 g/100g was close to the predicted value of 18.46 g/100g with minor deviation. Therefore, the model is considered valid to be employed in the optimization of protein extraction from cress seed.

3.6. Characterization of protein isolate

Sodium dodecyl sulfate-polyacrylamide gel electrophoresis (SDS-PAGE)

Electrophoretic separation of LSPI protein subunits was determined on 12% gradient SDS-PAGE (Fig. 3). It was found that LSPI is a complex protein consisting of albumin as a major component. The SDS-PAGE exhibited a number of bands with a molecular weight ranging from 250 kDa to 14 kDa that were consistently visible post silver staining.

Many legumes and oilseeds possess albumin and globulin as major protein fractions. It is reported that 11s globulin subunit in legume consists of an acid subunit between 21 and 25 kDa and the band between 28 and 40 kDa represents the basic subunit. The similar result was also observed in our work. Under the reduced condition, a comparable observation has been demonstrated in cumin [11] and sesame [22]. This indicates the formation of dimeric structure within the globulin protein is due to the inter-chain disulfide

bonds. In addition, the presence of protein bands ~ 47 and ~ 57 kDa were attributed to the 7s globulin protein indicating the absence of disulfide bond in protein subunits. This observation is in agreement with the previous report of Gokavi et al., 2004. Also the previous research on 7s protein has unfolded the fact that these subunits are prominently held by non-covalent, weak secondary forces, such as electrostatic forces, hydrogen bonding and hydrophobic (Siow & Gan, 2014).

As shown in Fig. 3, the presence of 2s albumin protein subunits < 18 kDa under a reduced condition is evident. According to Radovic et al., 1999, the polypeptide with MW size of 8–16 kDa is likely to be attributed to the presence of 2s albumin protein subunit. Further, cumin protein also shows the presence of 2s albumin subunit < 17 kDa under both reducing and non-reducing conditions [11].

3.6.1. Amino acid analysis

Table 4 summarizes the quantitative and qualitative composition of amino acids analyzed by HPLC. The result showed that Asp (9.23 ± 0.02) and Glu (23.33 ± 0.41) are the major non-essential amino acids, whereas Leu (7.60 ± 0.11) and Lys (6.17 ± 0.03) are the major essential amino acids present in the LSPI. A moderately higher quantity of Arg, Phe, Val, and Gly were also present. On the other hand Met and Cys, a sulfur-containing amino acid were found as a limiting amino acid. The observation is in close agreement with Gokavi et al., 2004 for garden cress. The similar result was also reported for melon seed, cumin seed, pumpkin seed and gourd seed (Siow & Gan, 2014).

Glu and Asp are acidic amino acids that exhibit excessive amounts of electrons which can be the ground of protein's strong antioxidant activity catered by donating electrons or scavenging the free radicals. In addition, the composition of Tyr, Met, His and Lys have been claimed to be accountable for demonstrating strong antioxidant effects [26]. Lysine also helps to maintain proper nitrogen balance. Moreover, Maus & Peters, 2017 reported that Glu can act as an excitatory neurotransmitter as well as an important part of sugar and fat metabolism. The protein sequence with Glu and Pro amino acid have also been reported to exhibit antidiabetic activity (Siow & Gan, 2014).

The characteristic amino acid profile of LSPI presented in Table 4 shows the presence of acidic, basic, uncharged polar and hydrophobic amino acids. The total essential amino acid percentage is 41.36%, indicating the potential of LSPI to be a significant resource for dietary essential amino acids. LSPI constituted more acidic amino acid when compared to the basic ones. The percentage of hydrophobic amino acids was found to be 30.27%, which facilitates their lipid target interaction or absorption into target organs via hydrophobic association which further imparts promising antioxidant potency [29]. A similar observation was also reported in cumin seed [11], and garden cress [23].

3.6.2. Fourier transform infrared spectroscopy (FTIR)

Figure 4a illustrated the secondary protein structure of LSPI recorded in the range of 500 to 4000 cm^{-1} . The peak in the region of 3400–3700 cm^{-1} is attributed to the O-H stretching, which was induced by flexural vibration frequencies of the intra- and intermolecular hydrogen bonds. The characteristic protein

band, amide I ($1600\text{--}1700\text{ cm}^{-1}$), amide II ($1500\text{--}1580\text{ cm}^{-1}$) and amide III ($1200\text{--}1400\text{ cm}^{-1}$) were observed in the IR spectrum of LSPI. These characteristic protein bands of amide I ($1600\text{--}1700\text{ cm}^{-1}$) and amide II ($1500\text{--}1580\text{ cm}^{-1}$) are attributed to the C = O stretching and N-H bending vibrations coupled to C-N stretching vibrations respectively. whereas amide III ($1200\text{--}1400\text{ cm}^{-1}$) band can be attributed to the complex mix of N-H bending, symmetric and asymmetric stretching of C-N and C-O-C along with a minor contribution from C-O in-plane bending and C-C stretching vibration [30].

In the present study, amide I ($1600\text{--}1700\text{ cm}^{-1}$) bands was deconvolved to get insight into the overlapping secondary structure of proteins which demonstrated that $1615\text{--}1638$, $1638\text{--}1645$, $1645\text{--}1662$, and $1662\text{--}1682\text{ cm}^{-1}$ corresponded to the β -sheet structure, random coil, α -helix structure, and β turn structure respectively [21]. The result exhibits the structure of LSPIs in the amide I band after peak shape fitting and area calculation. It shows that major secondary structure features in LSPI were 12.32% of β -sheets, 13.21% of α -helix, 16.06% of β -turns and 6.61% of β -antiparallel as well as 22.32% and 29.48% of protein aggregate 1 and 2 respectively (Table.5). The secondary structure of LSPI comprised of β structures majorly. The results obtained are in line with that of soybean [31], cottonseed meal [32], Australian chia seeds [20] and cumin seeds [11]. According to the Timilsena et al., 2016, the fall in β -sheets and a rise in β -turn, α -helix and random coil structures in chia seed protein is significantly due to denaturation of the protein. It has been also observed that high temperature and low pH significantly affect the secondary structure of a protein by converting the portion of the random coil into the β -turn and β -sheet [33].

3.6.3. SEM analysis

Surface morphological characteristics of LSPI particles is shown in Fig. 4b. The SEM micrograph exhibits that LSPI particle's surface are irregular and hydrophobic in nature. The result is in agreement with the amino acid composition of LSPI that indicated the presence of hydrophobic residues. According to Hou et al., 2017, surface hydrophobicity of protein are significantly affected by the presence of alkali concentration in the extraction procedure. The structure analysis also indicated the higher moisture diffusion of LSPI in an aqueous solution. Overall, the surface characteristics of the LSPI protein fraction contribute to the physicochemical and functional properties of the protein.

3.6.4. XRD analysis

Figure 4c shows the XRD pattern of the LSPI. It has been reported that solid food particles can be crystalline, semi-crystalline, or amorphous in nature. The diffractogram of LSPI between 5° to 80° with well-defined Bragg angles (2θ) shows two diffraction peaks at approximately 9.5 and 19.54° . The obtained XRD diffraction pattern is similar to that reported for chia protein isolate [21]. African yam beans exhibited diffraction peaks at 8.5° and 19.5° [34], whereas jackfruit seed protein reported at 8.5° , 19.5° and 24.5° [35]. Diffraction pattern depicts the partial crystalline nature of LSPI that can be attributed to the presence of disulfide linkages which impart a more ordered structure to the protein.

3.6.5. Thermal analysis

As shown in Fig. 4d, DSC reveals the structural and conformational properties of LSPI. The onset temperature (T_0), peak melting temperature (T_m), conclusion temperature (T_c) and enthalpy (ΔH) reveals the thermal stability of the LSPI, whereas ΔH describes the ratio of undenatured proteins and the extent of ordered structures. Shevkani et al., 2015 reported that thermal properties of a protein can also reflect the degree of the tertiary conformation. Figure 4d represents the endothermic peak of LSPI and T_0 , T_m , T_c , and ΔH were recorded to be 92.84 ± 1.42 , 120.37 ± 2.34 , 148.38 ± 1.86 and 225.75 ± 11.63 respectively. LSPI showed high T_m , which could be attributed to the high proportion of β -sheet conformations. These results are in agreement with the SDS-PAGE that indicates the presence of 7S globulin (β -sheet and random coil secondary structures). This subunit exhibits structural uniqueness and compactness of protein that possesses high thermal stability. In addition, higher hydrophobic nature of protein is attributed to the high T_m [37]. A similar observation was also reported for pea protein [38], soy protein [39], pearl millet [40] and red kidney bean [41]. Tang et al., 2009 suggested that ΔH values signifies low content of ordered secondary structures that influences the conformations of proteins during extraction. Furthermore, the fact that organic solvent can also induce the denaturation of protein needs to be considered.

3.6.6. Antioxidant property

The antioxidant potential of LSPI was determined by using DPPH, ABTS and FRAP assay [30]. DPPH and ABTS assay measured the free radical scavenging activity of the protein by donating hydrogen and breaking the chain reaction. In addition, FRAP assay evaluates the reduction potential of antioxidant proteins on ferric cyanide complexes (Fe^{3+}) to convert to ferrous form (Fe^{2+}). The results were validated with two controls, commercial soy protein isolate (SPI) and ascorbic acid (Table 6). It was observed that LSPI gave a lower antioxidant activity of 15.54% DPPH and 58.91% ABTS inhibition as well as $1.78 \mu M$ TE/mL antioxidant capacity than the ascorbic acid. The commercial SPI did not show any antioxidant activity. Siow & Gan, 2014 reported that the antioxidant capacity of protein isolate is reflected in the presence of functional amino acids within the protein structure. The result is in agreement with the amino acid composition of LSPI, which displays the presence of potential antioxidant amino acids such as Glu and Asp. This functional and bioactive amino acid exhibits a substantial pharmacological and therapeutic value due to their strong antioxidant potential [43].

3.6.7. α -Amylase inhibition activity

The percentage α -Amylase inhibition of LSPI was assayed and the value is displayed in Table 6. α -amylase hydrolyze the 1, 4- glycosidic linkage of polysaccharide that include starch and glycogen which generate glucose and maltose as a simple sugar molecule. Excess amount of simple sugar can lead to postprandial hyperglycemia [44]. LPSI induced inhibition of α -amylase can play a significant role in controlling hyperglycemia by delaying or limiting the digestion of carbohydrates. LSPI possesses a little inhibitory activity of α -amylase, approximately 8.5%. On the other hand, it was not detected in SPI. It has been reported that peptides derived from the native structure of soybean protein exhibit a functional amino acid residue that has a noticeable antidiabetic activity [45]. The protein sequence with Glu and Pro amino acid in LSPI might be the reason for antidiabetic activity [11, 46]. A similar result was also

obtained for those with cumin seed and barley protein isolate [11, 47]. Further research has to be carried out to examine the probable antidiabetic mechanisms of bioactive peptides derived from LSPI.

3.6.8. *In-vitro* protein digestibility (IVPD)

The % IVPD value of LSPI was estimated to be 73% as presented in Table 6. This result is in accordance with those reported on pea flour [48] and faba bean seed [49]. % IVPD previously reported for corn flour is 74%, whereas lupin and finger millet protein isolate exhibited higher values of 86.3–93.7% and 80–90% respectively [50]. The possible reasons for the low digestibility of plant-derived protein could be low protein solubility as well as the presence of antinutritional factors such as phytates and tannins, that limit the digestive enzyme accessibility to the protein bodies [51]. Previous report suggests that % of IVPD increases while cooking, soaking or dehulling and hydrothermal treatment degrades the anti-nutritional factors along with denaturation of native protein during processing steps thereby rendering the protein bodies more accessible to digestive enzymes [50].

3.6.9. Effect of pH and salt on protein solubility

The solubility of LSPI was evaluated as a function of increasing pH (Fig. 5). Protein solubility at various pH, indicates their characteristics and functional features which decides their application in food product development. In addition, texture, colour and the sensory properties of a product are predominantly affected by the nature of protein present in them. Timilsena et al., 2016 reported that solubility of the protein importantly contributes to the emulsification, foaming, and gelation that significantly affect their application in the formulation. The LSPI showed diverse solubility profiles at pH 2.0–11.0, demonstrating a U-shaped curve. Lower solubility was observed at isoelectric point ($pI = 4.5$) whereas significant ($p < 0.05$) solubility was recorded with change in pH higher or lower than the pI . According to Ulloa et al., 2017, isoelectric pH values for many plant-based proteins are observed in the range of 4 and 5 at which no net charge is present on the protein. As the pH decreases, the repulsive forces increase due to the presence of large net charges. Protein solubility manifests its ability to interact with water due to their surface hydrophobic and hydrophilic characteristics that are significantly affected by the amino acids composition as well as native or denatured state of the proteins [53]. These results indicate that LSPI has good solubility under basic conditions. Comparable results were obtained for pea protein isolate with least solubility at pH 5.0 [54] as well as for chia seed [20] and cashew nut [55]. Protein solubility of *Sesamum indicum* seeds have been also reported to be better in basic range [56].

3.6.10. Analysis of Bulk density, water holding (WHC) and oil absorption capacity (OAC)

Table 7 represents the value of bulk density, WHC, and OAC of LSPI. Bulk density reflects the mass of particles which has economic and functional significance. WHC represents the water that is absorbed and retained by the protein, whereas OAC shows the binding of fat to the non-polar side chain of the protein. Both WHC and OAC significantly influence the characteristics of the formulated food product in terms of texture, colour and sensory properties [32].

The bulk density value of LSPI was recorded to be approximately 0.62 g/cm² which was higher when compared to soy protein isolate (0.56 g/cm²). Similar values are reported for mung bean isolates (0.55 g/cm²) whereas our bulk density value was lower than cowpea (0.71 g/cm²) and pea protein (0.68 g/cm²) [57]. It has been seen that a lower value of bulk density attributes to the high occluded air content that improves flowability and instant favors solubilization. On the other hand, higher bulk density in certain food formulations have been found suitable in convalescent and child feeding [58].

The WHC of LSPI was determined to be 3.1 mL/g, which was higher than the market sample soy protein isolate i.e., 2.8 mL/g. The higher WHC of protein isolate indicates the presence of a high number of the polar group that interferes with water molecules to augment the hydration of proteins [59]. A similar observation was also noted in fenugreek protein concentrate (1.56 mL/g) [60], bitter lupin protein isolate (2.12 mL/g) [43].

The OAC value of soy protein isolate was evaluated to be 1.54 mL/g which was higher than the value of LSPI calculated as 1.70 mL/g. This could be attributed to the binding of various non-polar side chains to the hydrocarbon chains of fats and the subsequent higher oil absorption. A similar observation was made with chickpea and soy protein isolates which showed an oil absorption capacity of 1.7 mL/g and 1.9 mL/g respectively.

3.6.11 Emulsifying activity index (EAI) and emulsion stability (ES)

The EAI (m²/g) and ES (min) measures the emulsion capacity and the stability of LSPI at 100, 150 and 200 mg concentration as a function of pH (Fig. 6). Protein molecule possesses its emulsifying property due to its surface hydrophilic-lipophilic characteristics which are significantly influenced by nonpolar amino acids, charged amino acids and non-charged polar amino acids composition. As an emulsifier, it exhibits the ability to lower the tension at the oil-water interfaces that control the formation of adsorption layer diffusion and the aggregation of oil droplets [21]. The diffusion is prominently influenced by protein concentration, molecular size, temperature, pH, ionic strength, and solubility. In our study, the lowest value of ESI and ES was observed at pH 4.5 that can be attributed to the lower solubility of the protein. On the other hand, the ESI and ES for LSPI were found to be greater at pH values higher or lower than the pI, which suggests the pH had a significant influence on the ESI and ES property of LSPI. These observations are in close proximity to those reported in rice bran protein [21, 61] and safflower protein isolate [62].

3.6.12 Foaming capacity (FC) and Foaming stability (FS)

Foaming properties (FC and FS) are critical in many aspects during formulation of the various food systems. It also indicates their suitability in food for aeration and whipping which is mainly associated with the two-phase interface. The FC and FS of LSPI dispersions at 30, 60 and 90 mg concentration were observed as a pH with pH and time (min) dependent respectively, as shown in Fig. 7. Protein molecules due to their hydrophobic and hydrophilic properties utilize uniform distribution of air cells which provide a continuous inter-molecular cohesiveness and elasticity to the air bubble in the structure of foods [21]. In

our study, the foaming capacity was found to be minimum in the range of pH 4.0–7.0 and the lowest value was at pH 4.5 (pI) for all the concentrations. The FC and FS of the LSPI were slightly increased towards the acidic range below pI, and major increase towards basic pH condition and reached maximum at pH 11. This result was in agreement with the solubility profile of a market sample of SPI. Increasing foam value may be due to the greater solubility and increased net charges of LSPI where the hydrophobic interactions are weak and surface activity with flexibility of protein is increased. Timilsena et al., 2016 reported that surface activity and flexibility allow protein molecules to partially unfold at the air/water interface that encapsulates air particles and enhances the foam formation. In addition, protein particles in dispersion stabilize the foams as a result of being positioned at the air/water interface and serve as a physical barrier to bubble coalescence. These results obtained in the study are comparable with those with chia seed [20] and kidney bean [36]. The contradictory studies is also reported for guava seed [63] that demonstrates higher FC and FS at acidic pH.

4. Conclusion

The findings of this study present *Lepidium sativum* seed cake as a potential source for production of protein isolate, that is optimized by RSM effectively. The finest environments were alkali concentration of 0.17 M, buffer to sample ratio of 1/45 (w/v), extraction time of 45 min and an extraction temperature of 26°C with the highest protein yield of 19%. The LSPI shows fine balance of essential amino acids and functional properties in terms of its water and oil binding capacity, protein solubility, emulsification and foaming. Additionally, significant antioxidant activity and anti-diabetic activity was also recorded. Therefore, LSPI could be an ideal and novel source of protein in food systems that can serve as a promising nutraceutical and functional food ingredient.

Declarations

Funding:

No funding was received for conducting this study

Conflict of Interest:

On behalf of all authors, the corresponding author states that there is no conflict of interest.

Competing Interest:

The authors have no competing interests to declare that are relevant to the content of this article.

Ethical Approval:

Not applicable

Consent to Participate:

Not applicable

Consent for publication:

All authors unanimously agree for submission of the manuscript to this journal

Data Availability Statement:

All data generated or analyzed during this study are included in this published article

Code availability:

Not applicable

Acknowledgments:

The authors are thankful for the Basic Scientific Research Fellowship in Sciences by the University Grants Commission, Government of India, for providing financial assistance (Grant number: 2812/UGC-SAP) during this investigation.

References

1. Ismail BP, Senaratne-Lenagala L, Stube A, Brackenridge A (2020) Protein demand: review of plant and animal proteins used in alternative protein product development and production. *Anim Front Rev Mag Anim Agric* 10:53–63. <https://doi.org/10.1093/af/vfaa040>
2. Hertzler SR, Lieblein-Boff JC, Weiler M, Allgeier C (2020) Plant Proteins: Assessing their nutritional quality and effects on health and physical function. *Nutrients* 12:3704. <https://doi.org/10.3390/nu12123704>
3. Satija A, Hu FB (2018) Plant-based diets and cardiovascular health. *Trends Cardiovasc Med*. <https://doi.org/10.1016/j.tcm.2018.02.004>
4. Williams KA, Patel H (2017) Healthy Plant-Based Diet: What does it really mean? *J Am Coll Cardiol* 70:423–425. <https://doi.org/10.1016/j.jacc.2017.06.006>
5. Kadam D, Lele SS (2018) Value addition of oilseed meal: a focus on bioactive peptides. *J Food Meas Charact* 12:449–458. <https://doi.org/10.1007/s11694-017-9658-3>
6. Dixit JR III V, Kumar I, Palandurkar K, et al (2020) *Lepidium sativum*: Bone healer in traditional medicine, an experimental validation study in rats. *J Fam Med Prim Care* 9:812–818. https://doi.org/10.4103/jfmprc.jfmprc_761_19
7. Singh CS, Paswan VK (2017) The potential of Garden Cress (*Lepidium sativum* L.) seeds for development of functional foods. *IntechOpen*
8. Kadam D, Palamthodi S, Lele SS (2018) LC-ESI-Q-TOF-MS/MS profiling and antioxidant activity of phenolics from *L. Sativum* seedcake. *J Food Sci Technol* 55:1154–1163. <https://doi.org/10.1007/s13197-017-3031-8>

9. Engy et al (2021) Characterization of Garden Cress mucilage and its prophylactic effect against indomethacin-induced enterocolitis in rats. *Biointerface Res Appl Chem* 11:13911–13923. <https://doi.org/10.33263/BRIAC116.1391113923>
10. Sonawane SK, Arya SS (2018) Plant Seed Proteins: Chemistry, Technology and Applications. *Curr Res Nutr Food Sci J* 6:461–469
11. Siow H, Gan C (2014) Functional protein from cumin seed (*Cuminum cyminum*): Optimization and characterization studies. *Food Hydrocoll* 41:178–187. <https://doi.org/10.1016/j.foodhyd.2014.04.017>
12. Kusuma HS, Mahfud M (2016) Response surface methodology for optimization studies of microwave- assisted extraction of Sandalwood Oil. 14
13. Vishwasrao C, Chakraborty S, Ananthanarayan L (2017) Partial purification, characterisation and thermal inactivation kinetics of peroxidase and polyphenol oxidase isolated from Kalipatti sapota (*Manilkara zapota*). *J Sci Food Agric* 97:3568–3575. <https://doi.org/10.1002/jsfa.8215>
14. Gratzfeld-Huesgen A (1999) Sensitive and reliable amino acid analysis in protein hydrolysates using the Agilent 1100 Series HPLC. Agil Technol Publ Number 5968-5658E
15. Sonawane SK, Arya SS (2017) *Citrullus lanatus* protein hydrolysate optimization for antioxidant potential. *J Food Meas Charact* 11:1834–1843. <https://doi.org/10.1007/s11694-017-9565-7>
16. Kadam D, Lele SS (2018) Cross-linking effect of polyphenolic extracts of *Lepidium sativum* seedcake on physicochemical properties of chitosan films. *Int J Biol Macromol* 114:1240–1247. <https://doi.org/10.1016/j.ijbiomac.2018.04.018>
17. Pérez-Ramírez IF, Castaño-Tostado E, Ramírez-De León JA, et al (2015) Effect of stevia and citric acid on the stability of phenolic compounds and in vitro antioxidant and antidiabetic capacity of a roselle (*Hibiscus sabdariffa L.*) beverage. *Food Chem* 172:885–892. <https://doi.org/10.1016/j.foodchem.2014.09.126>
18. Phongthai S, Lim S, Rawdkuen S (2016) Optimization of microwave-assisted extraction of rice bran protein and its hydrolysates properties. *J Cereal Sci* 70:146–154. <https://doi.org/10.1016/j.jcs.2016.06.001>
19. Mehta V, Sharma A, Tanwar S, Malairaman U (2016) In vitro and in silico evaluation of the antidiabetic effect of hydroalcoholic leaf extract of *Centella asiatica*. *Int J Pharm Pharm Sci* 8:357–362
20. Timilsena YP, Adhikari R, Barrow CJ, Adhikari B (2016) Physicochemical and functional properties of protein isolate produced from Australian chia seeds. *Food Chem* 212:648–656. <https://doi.org/10.1016/j.foodchem.2016.06.017>
21. Hou F, Ding W, Qu W, et al (2017) Alkali solution extraction of rice residue protein isolates: Influence of alkali concentration on protein functional, structural properties and lysinoalanine formation. *Food Chem* 218:207–215. <https://doi.org/10.1016/j.foodchem.2016.09.064>
22. Orruño E, Morgan MRA (2007) Purification and characterisation of the 7S globulin storage protein from sesame (*Sesamum indicum L.*). *Food Chem* 100:926–934.

<https://doi.org/10.1016/j.foodchem.2005.10.051>

23. Gokavi SS, Malleshi NG, Guo M (2004) Chemical composition of garden cress (*Lepidium sativum*) seeds and its fractions and use of bran as a functional ingredient. *Plant Foods Hum Nutr* 59:105–111. <https://doi.org/10.1007/s11130-004-4308-4>
24. Radovic RS, Maksimovic R V., Brkljacic MJ, et al (1999) 2S albumin from buckwheat (*Fagopyrum esculentum Moench*) seeds. *J Agric Food Chem* 47:1467–1470. <https://doi.org/10.1021/jf980778s>
25. Olaofe O, Adeyemi FO, Adediran GO (1994) Amino acid and mineral compositions and functional properties of some oilseeds. *J Agric Food Chem* 42:878–881. <https://doi.org/10.1021/jf00040a007>
26. Matemu A, Nakamura S, Katayama S (2021) Health Benefits of antioxidative peptides derived from legume proteins with a high amino acid score. *antioxidants* 10:316. <https://doi.org/10.3390/antiox10020316>
27. Maus A, Peters GJ (2017) Glutamate and α -ketoglutarate: key players in glioma metabolism. *Amino Acids* 49:21–32. <https://doi.org/10.1007/s00726-016-2342-9>
28. Gault VA, O'Harte FPM, Harriott P, Flatt PR (2002) Characterization of the cellular and metabolic effects of a novel enzyme-resistant antagonist of glucose-dependent insulinotropic polypeptide. *Biochem Biophys Res Commun* 290:1420–1426. <https://doi.org/10.1006/bbrc.2002.6364>
29. Zou T-B, He T-P, Li H-B, et al (2016) The Structure-Activity Relationship of the Antioxidant Peptides from Natural Proteins. *Molecules* 21:72. <https://doi.org/10.3390/molecules21010072>
30. Kadam D, Shah N, Palamthodi S, Lele SS (2018) An investigation on the effect of polyphenolic extracts of *Nigella sativa* seedcake on physicochemical properties of chitosan-based films. *Carbohydr Polym* 192:347–355. <https://doi.org/10.1016/j.carbpol.2018.03.052>
31. Song CL, Zhao XH (2014) Structure and property modification of an oligochitosan-glycosylated and crosslinked soybean protein generated by microbial transglutaminase. *Food Chem* 163:114–119. <https://doi.org/10.1016/j.foodchem.2014.04.089>
32. Du M, Xie J, Gong B, et al (2018) Extraction, physicochemical characteristics and functional properties of Mung bean protein. *Food Hydrocoll* 76:131–140. <https://doi.org/10.1016/j.foodhyd.2017.01.003>
33. Diniz RS, Coimbra JS dos R, Teixeira ÁVN de C, et al (2014) Production, characterization and foamability of α -lactalbumin/glycomacropeptide supramolecular structures. *Food Res Int* 64:157–165. <https://doi.org/10.1016/j.foodres.2014.05.079>
34. Arogundade LA, Mu TH, Akinhanmi TF (2016) Erratum: Corrigendum to 'Structural, physicochemical and interfacial stabilisation properties of ultrafiltered African yam bean (*Sphenostylis stenocarpa*) protein isolate compared with those of isoelectric protein isolate' (*LWT - Food Science and Technol*. *LWT - Food Sci Technol* 73:715–716. <https://doi.org/10.1016/j.lwt.2016.03.017>
35. Haque MA, Akter F, Rahman H, Baqui MA (2020) Jackfruit seeds protein isolate by spray drying method: the functional and physicochemical characteristics. *Food Nutr Sci* 11:355. <https://doi.org/10.4236/fns.2020.115026>

36. Shevkani K, Singh N, Kaur A, Rana JC (2015) Structural and functional characterization of kidney bean and field pea protein isolates: A comparative study. *Food Hydrocoll* 43:679–689. <https://doi.org/10.1016/j.foodhyd.2014.07.024>
37. Panja AS, Bandopadhyay B, Maiti S (2015) Protein thermostability is owing to their preferences to non-polar smaller volume amino acids, variations in residual physico-chemical properties and more salt-bridges. *PLoS ONE* 10:e0131495. <https://doi.org/10.1371/journal.pone.0131495>
38. He XH, Liu HZ, Liu L, et al (2014) Effects of high pressure on the physicochemical and functional properties of peanut protein isolates. *Food Hydrocoll* 36:123–129. <https://doi.org/10.1016/j.foodhyd.2013.08.031>
39. Hua Y, Cui SW, Wang Q, et al (2005) Heat induced gelling properties of soy protein isolates prepared from different defatted soybean flours. *Food Res Int* 38:377–385. <https://doi.org/10.1016/j.foodres.2004.10.006>
40. Agrawal H, Joshi R, Gupta M (2016) Isolation, purification and characterization of antioxidative peptide of pearl millet (*Pennisetum glaucum*) protein hydrolysate. *Food Chem* 204:365–372. <https://doi.org/10.1016/j.foodchem.2016.02.127>
41. Rui X, Boye JI, Ribereau S, et al (2011) Comparative study of the composition and thermal properties of protein isolates prepared from nine *Phaseolus vulgaris* legume varieties. *Food Res Int* 44:2497–2504. <https://doi.org/10.1016/j.foodres.2011.01.008>
42. Tang CHE, Wang XY, Liu F, Wang CS (2009) Physicochemical and conformational properties of buckwheat protein isolates: Influence of polyphenol removal with cold organic solvents from buckwheat seed flours. *J Agric Food Chem* 57:10740–10748. <https://doi.org/10.1021/jf901928h>
43. Duranti M, Consonni A, Magni C, et al (2008) The major proteins of lupin seed: Characterisation and molecular properties for use as functional and nutraceutical ingredients. *Trends Food Sci Technol* 19:624–633. <https://doi.org/10.1016/j.tifs.2008.07.002>
44. Hiyoshi T, Fujiwara M, Yao Z (2019) Postprandial hyperglycemia and postprandial hypertriglyceridemia in type 2 diabetes. *J Biomed Res* 33:1–16. <https://doi.org/10.7555/JBR.31.20160164>
45. Lu J, Zeng Y, Hou W, et al (2012) The soybean peptide aglycin regulates glucose homeostasis in type 2 diabetic mice via IR/IRS1 pathway. *J Nutr Biochem* 23:1449–1457. <https://doi.org/10.1016/j.jnutbio.2011.09.007>
46. Srinivasan V, Radhakrishnan S, Angayarkanni N, Sulochana KN (2019) Antidiabetic effect of free amino acids supplementation in human visceral adipocytes through adiponectin-dependent mechanism. *Indian J Med Res* 149:41–46. https://doi.org/10.4103/ijmr.IJMR_1782_16
47. Alu'Datt MH, Ereifej K, Abu-Zaiton A, et al (2012) Anti-oxidant, anti-diabetic, and anti-hypertensive effects of extracted phenolics and hydrolyzed peptides from barley protein fractions. *Int J Food Prop* 15:781–795. <https://doi.org/10.1080/10942912.2010.503357>
48. Bamidele OP, Akanbi CT (2013) Influence of gamma irradiation on the nutritional and functional properties of pigeon pea (*Cajanus cajan*) flour. *Afr J Food Sci* 7:285–290.

<https://doi.org/10.5897/AJFS2013>.

49. Osman AMA, Hassan AB, Osman GAM, et al (2014) Effects of gamma irradiation and/or cooking on nutritional quality of faba bean (*Vicia faba L.*) cultivars seeds. J Food Sci Technol 51:1554–1560. <https://doi.org/10.1007/s13197-012-0662-7>
50. Annor GA, Tyl C, Marcone M, et al (2017) Why do millets have slower starch and protein digestibility than other cereals? Trends Food Sci Technol 66:73–83. <https://doi.org/10.1016/j.tifs.2017.05.012>
51. Samtiya M, Aluko RE, Dhewa T (2020) Plant food anti-nutritional factors and their reduction strategies: an overview. Food Prod Process Nutr 2:6. <https://doi.org/10.1186/s43014-020-0020-5>
52. Ulloa JA, Villalobos Barbosa MC, Resendiz Vazquez JA, et al (2017) Production, physico-chemical and functional characterization of a protein isolate from jackfruit (*Artocarpus heterophyllus*) seeds. CyTA - J Food 15:497–507. <https://doi.org/10.1080/19476337.2017.1301554>
53. Saetae D, Kleekayai T, Jayasena V, Suntornsuk W (2011) Functional properties of protein isolate obtained from physic nut (*Jatropha curcas L.*) seed cake. Food Sci Biotechnol 20:29–37. <https://doi.org/10.1007/s10068-011-0005-x>
54. Li C, Xue H, Chen Z, et al (2014) Comparative studies on the physicochemical properties of peanut protein isolate-polysaccharide conjugates prepared by ultrasonic treatment or classical heating. Food Res Int 57:1–7. <https://doi.org/10.1016/j.foodres.2013.12.038>
55. Ogunwolu SO, Henshaw FO, Mock HP, et al (2009) Functional properties of protein concentrates and isolates produced from cashew (*Anacardium occidentale L.*) nut. Food Chem 115:852–858. <https://doi.org/10.1016/j.foodchem.2009.01.011>
56. Fasuan TO, Gbadamosi SO, Omobuwajo TO (2018) Characterization of protein isolate from *Sesamum indicum* seed: In vitro protein digestibility, amino acid profile, and some functional properties. Food Sci Nutr 6:1715–1723. <https://doi.org/10.1002/fsn3.743>
57. Butt M, Batool R (2010) Nutritional and functional properties of some promising legumes protein isolates. Pak J Nutr 9:373–379. <https://doi.org/10.3923/pjn.2010.373.379>
58. Chandra S, Singh S, Kumari D (2015) Evaluation of functional properties of composite flours and sensorial attributes of composite flour biscuits. J Food Sci Technol 52:3681–3688. <https://doi.org/10.1007/s13197-014-1427-2>
59. Petukhov M, Rychkov G, Firsov L, Serrano L (2004) H-bonding in protein hydration revisited. Protein Sci Publ Protein Soc 13:2120–2129. <https://doi.org/10.1110/ps.04748404>
60. El Nasri NA, El Tinay AH (2007) Functional properties of fenugreek (*Trigonella foenum graecum*) protein concentrate. Food Chem 103:582–589. <https://doi.org/10.1016/j.foodchem.2006.09.003>
61. Zhang H-J, Zhang H, Wang L, Guo X-N (2012) Preparation and functional properties of rice bran proteins from heat-stabilized defatted rice bran. Food Res Int 47:359–363. <https://doi.org/10.1016/j.foodres.2011.08.014>
62. Ulloa JA, Rosas-Ulloa P, Ulloa-Rangel BE (2011) Physicochemical and functional properties of a protein isolate produced from safflower (*Carthamus tinctorius L.*) meal by ultrafiltration. J Sci Food Agric 91:572–577. <https://doi.org/10.1002/jsfa.4227>

63. Bernardino Nicanor, A.Ortiz Moreno ALMA y GDO (2001) Guava Seed Protein Isolate: Functional and nutritional characterization. J Food Biochem 25:77–90

Tables

Table 1: Proximate composition of garden cress seed flour.

Component	Composition (g/100g)
Moisture	9.62 ± 0.17
Crude oil	3.21 ± 0.29
Crude protein	28.25 ± 0.14
Total ash	4.91 ± 0.20
Crude carbohydrate	54.26

Data correspond to the mean ± SD of three experiments.

Table 2 and 3 is available in the Supplementary Files section.

Table 4: Amino acid composition and percentage of an amino acid with different characteristics in LSPI (per 1000 residues)

Amino Acid	Percentage composition of amino acid in seedcake	FAO/WHO/UNU daily EAA requirement
Essential acid		
Threonine	4.10±0.08	15
Methionine	0.78±0.02	10.4
Cysteine	0.17±0.1	4.1
Isoleucine	4.90±0.04	20
Leucine	7.60±0.11	39
Phenylalanine	5.49±0.17	25
Tyrosine	2.58±0.09	
Histidine	3.73±0.09	10
Lysine	6.17±0.015	30
Valine	5.84±0.14	26
Tryptophan	-	4
Non-Essential amino acid		
Aspartic acid	9.23±0.02	
Serine	4.32±0.04	
glutamic acid	23.33±0.41	
Glycine	5.02±0.07	
Proline	4.71±0.06	
Alanine	4.32±0.21	
Tyrosine	2.58±0.09	
Arginine	7.71±0.021	
Percentage of an amino acid with different characteristics		
Acidic	32.56	
Basic	17.07	
Hydrophobic	30.27	
Uncharged polar	16.19	

Total essential amino acid	41.36
Total nonessential amino acid	59.64

Data correspond to the mean \pm SD of three experiments.

Acidic: Aspartic acid, glutamic acid; Basic: Lysine, arginine, histidine; Hydrophobic: Alanine, isoleucine, leucine, methionine, phenylalanine, proline, valine; Uncharged polar: Glycine, serine, threonine, tyrosine, cysteine.

Table 5: Secondary structure of LSPI protein isolate

The relative content of the secondary structural feature	<i>L. sativum</i> (%)
Protein aggregates 1	22.324
β -sheets	12.321
α -helix	13.214
β -turns	16.062
β -Antiparallel	6.602
Protein aggregates 2	22.324

Data corresponds to the mean \pm SD of three experiments.

Table 6: In-vitro antioxidant, antidiabetic activity and protein digestibility of *Lepidium sativum* protein isolate (LSPI).

Sample	Antioxidant activity (IC 50)			Protein digestibility	Antidiabetic activity
	DPPH (% of inhibition)	ABTS (% of inhibition)	FRAP (TE/mL)		
LSPI	15.54 \pm 2.45	58.91 \pm 1.31	1.78 \pm 2.62	73%	8.5 \pm 0.21
SPI	ND	ND	ND	82%	ND
Standard (TE)	28.32 (5 μ g/mL)	12.42 (5 μ g/mL)			Not determined

Data correspond to the mean \pm SD of three experiments.

Table 7: The physicochemical property of LSPI protein isolate

Physicochemical property

	Bulk density (g/mL)	Water absorption capacity (mL/g)	Oil absorption capacity (mL/g)
LSPI	0.62±0.02	3.1±0.24	1.70±0.15
Soy protein isolate	0.51±0.02	2.8±0.11	1.54±0.03

Data correspond to the mean ± SD of three experiments.

Figures

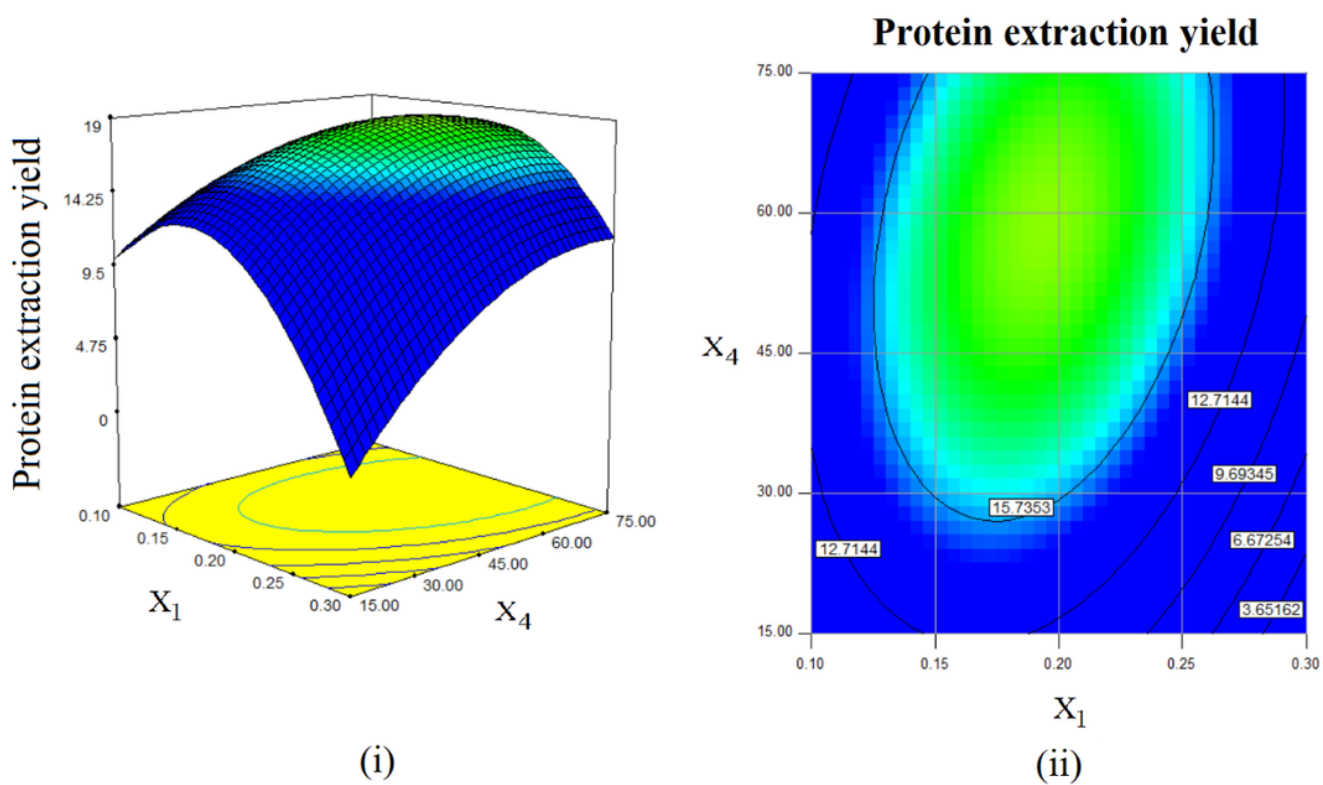


Figure 1

Response surface: (i) three-dimensional plots and (ii) contour plot for protein as a function of alkali concentration (X_1) and extraction temperature (X_4)

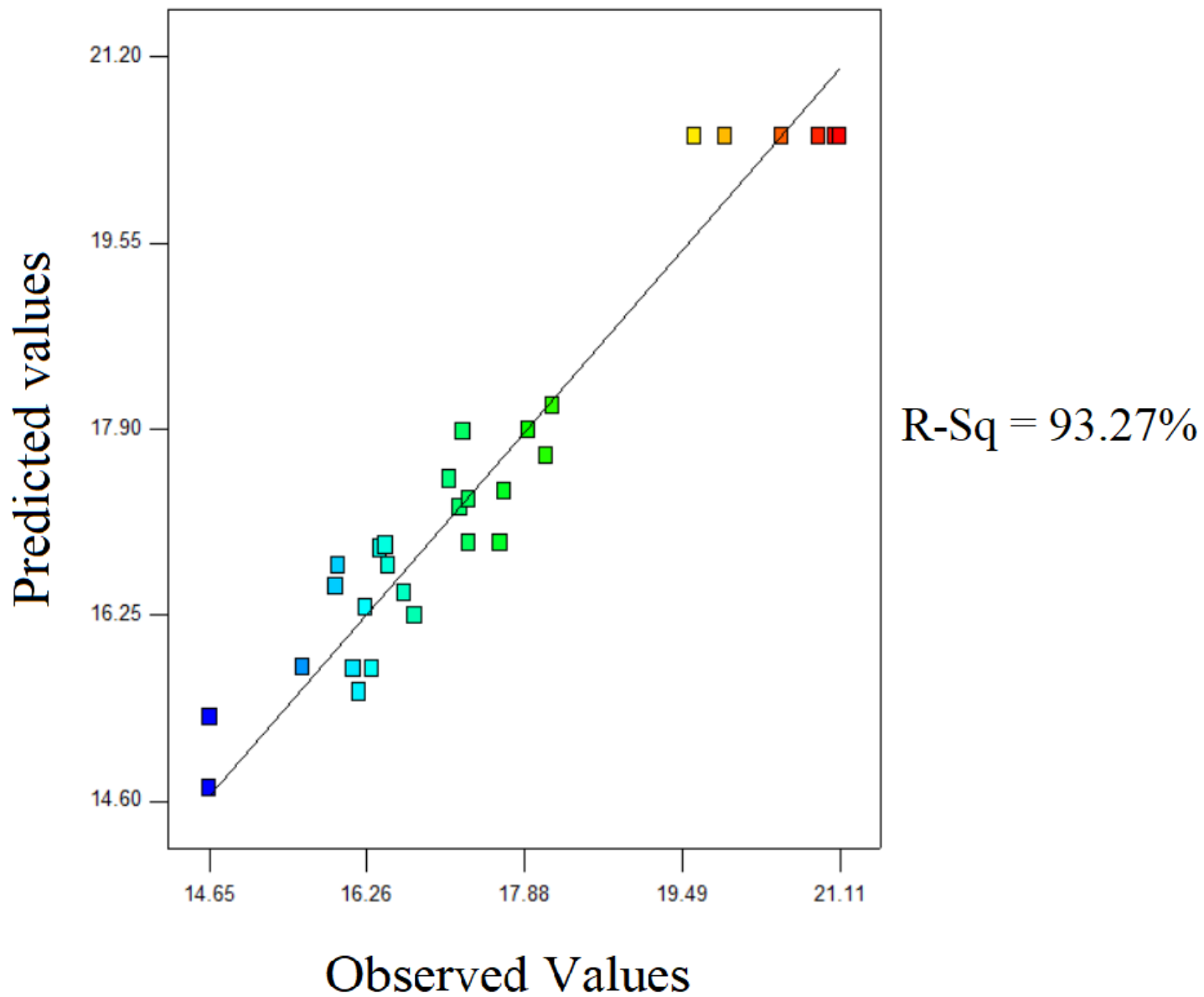


Figure 2

Comparison between observed and predicted values of protein yield (%)

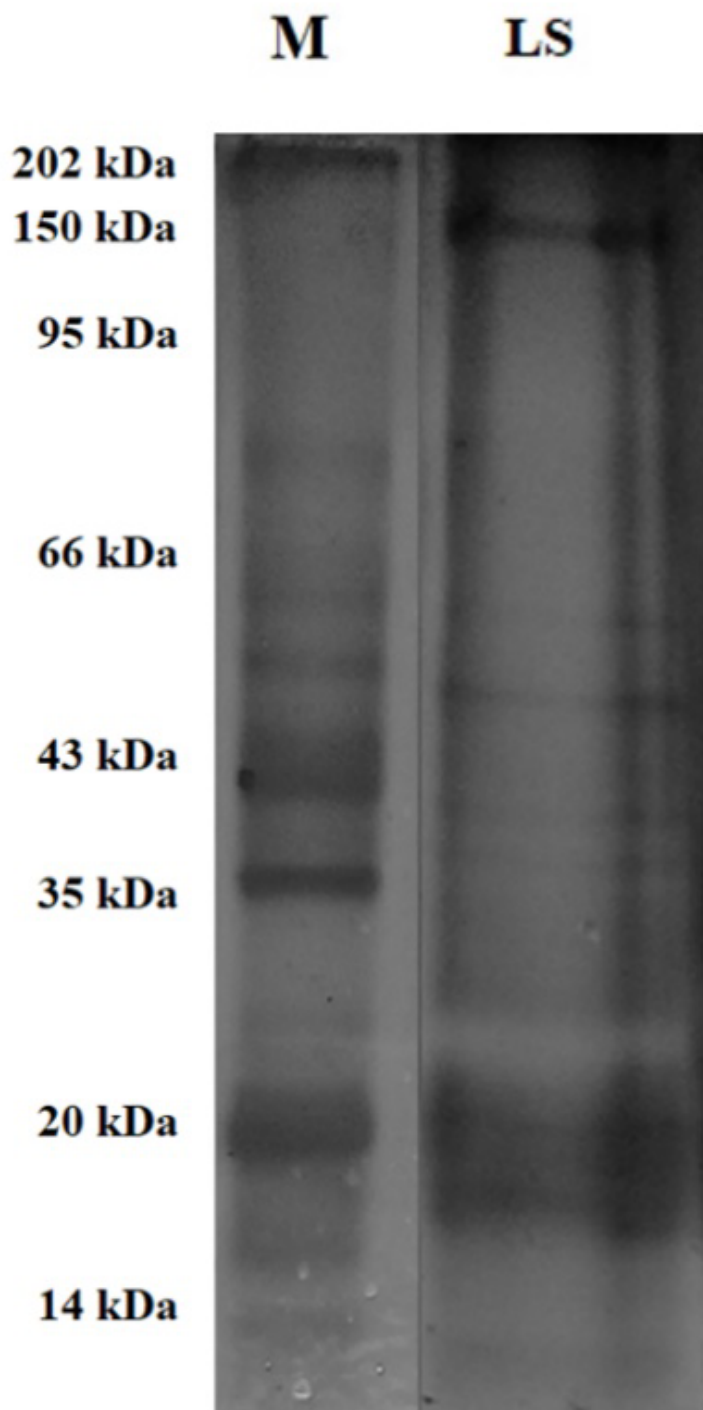
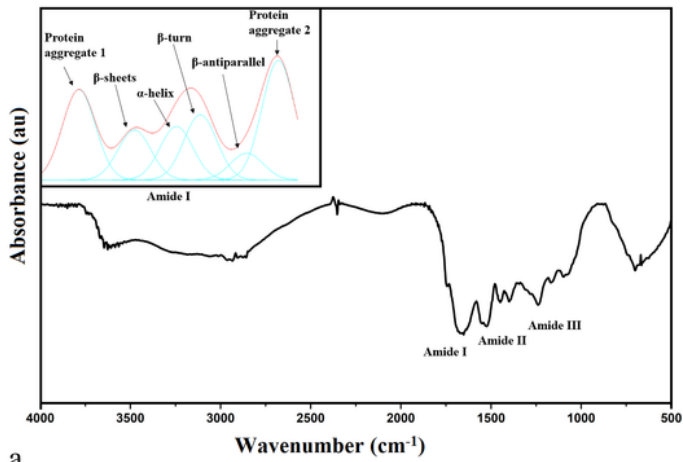
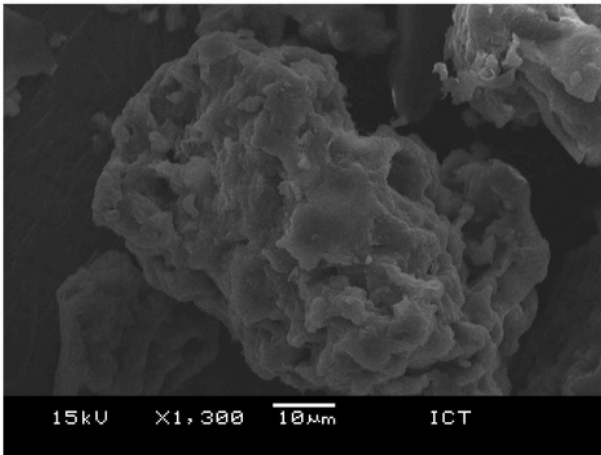


Figure 3

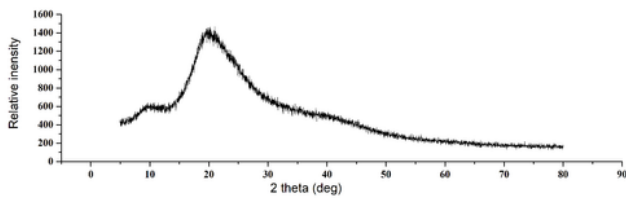
Electrophoretic separation of protein subunits of garden cress seedcake flour on 12 % SDS-PAGE.



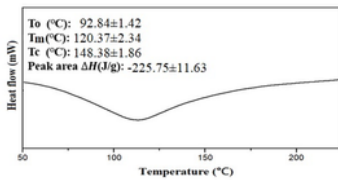
a



b



c



d

Figure 4

(a) Fourier transform infrared spectroscopy (FTIR) (cm⁻¹) of *Lepidium sativa protein isolate* (LSPI). (b) SEM analysis of *Lepidium sativum* protein isolate (LSPI). (c) X-Ray Diffraction (XRD) analysis of *Lepidium sativum* protein isolates (LSPI) (d) Thermal analysis

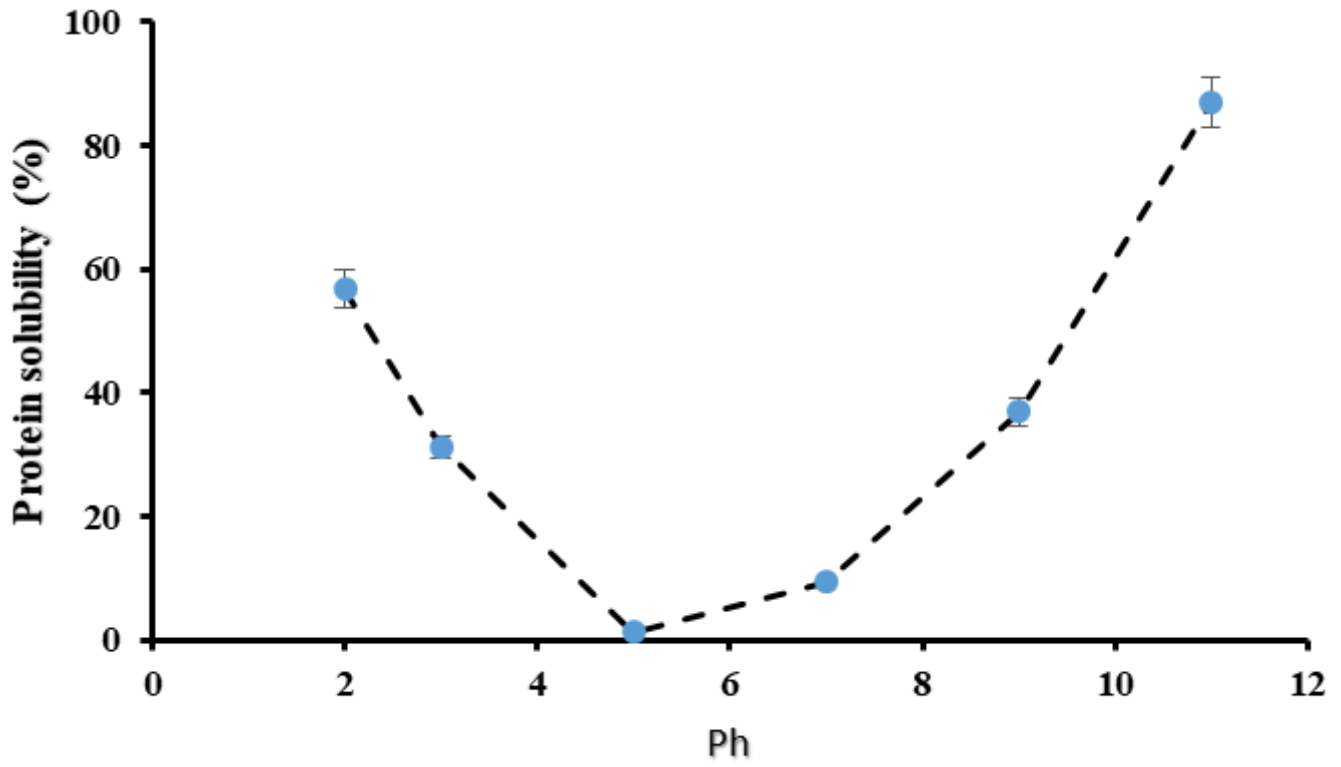


Figure 5

Solubility of *Lepidium sativa* protein isolate (LSPI) as a function of pH. Data are the mean \pm standard deviation of three replicates. Mean values labeled with different letters are significantly different ($p < 0.05$)

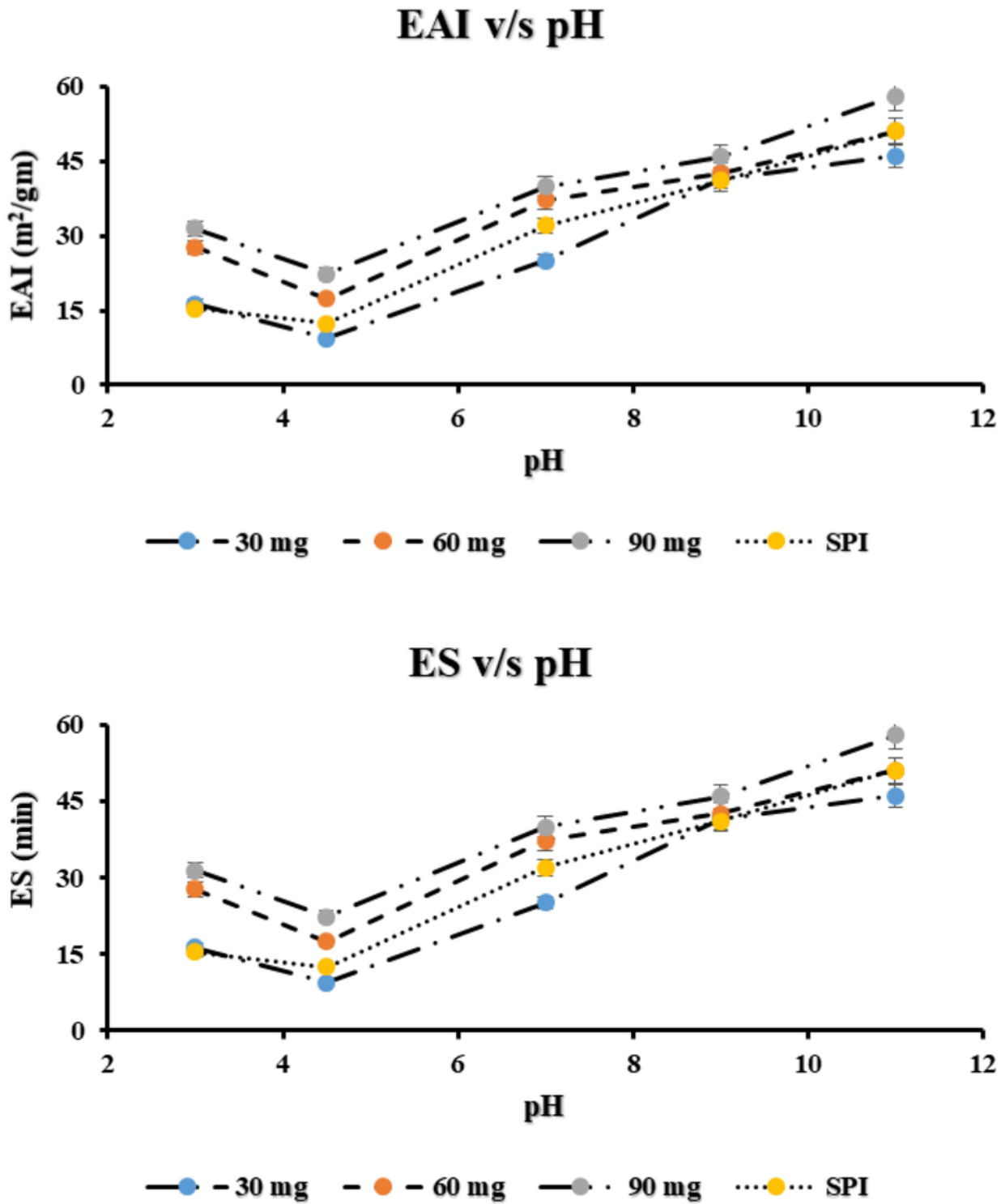


Figure 6

(a) Emulsion capacity index and (b) Emulsion stability of *Lepidium sativa* protein isolate (LSPi) as a function of pH and concentration. Data correspond to the mean \pm SD of three experiments.

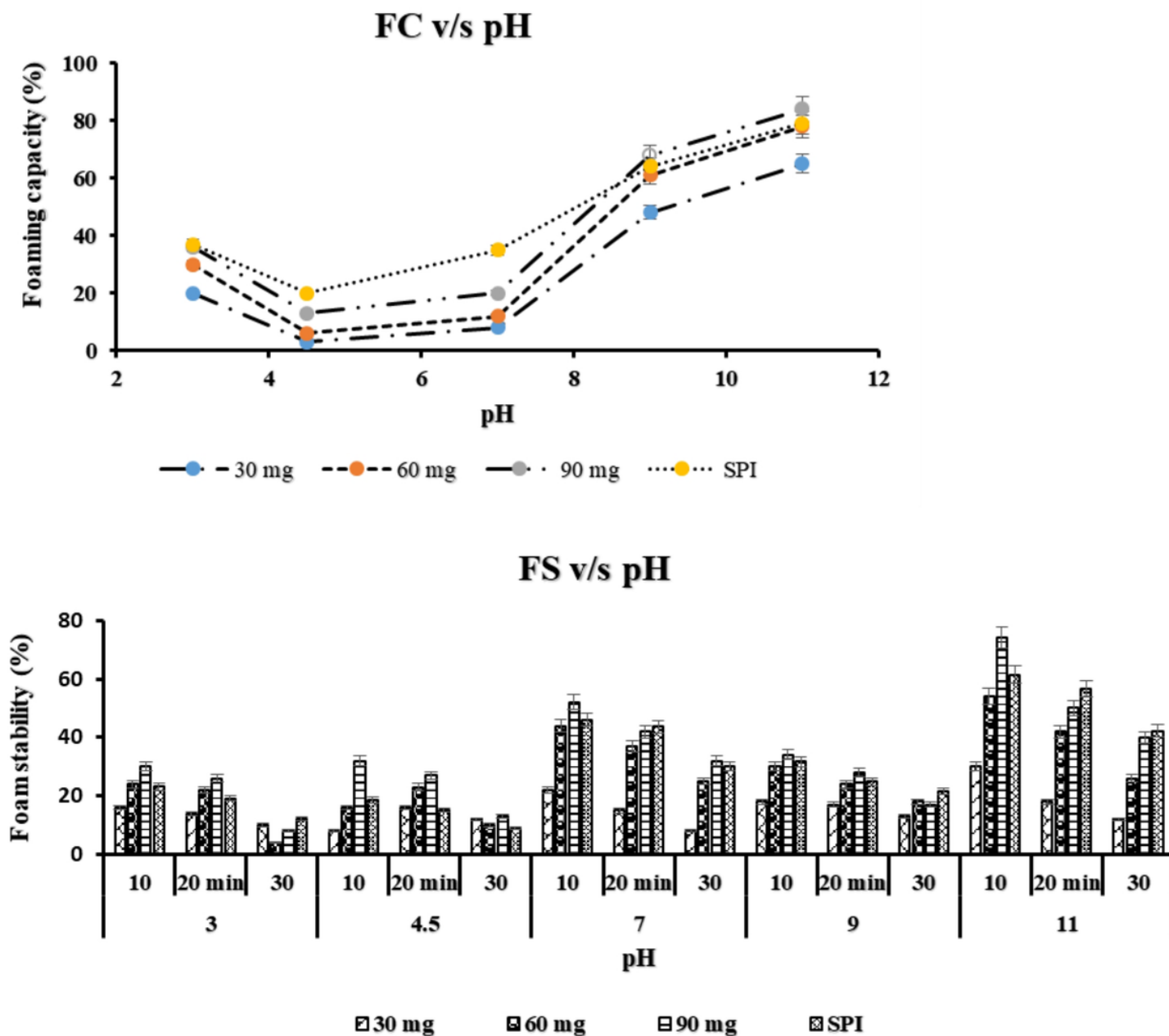


Figure 7

(a) Foaming capacity as a function of pH and concentration. (b) Foaming stability of *Lepidium sativa* protein isolate (LSPI) as a function of pH, time and concentration. Data correspond to the mean \pm SD of three experiments.

Supplementary Files

This is a list of supplementary files associated with this preprint. Click to download.

- [Table2and3.docx](#)